Nanoporous Thermochromic VO2 (M) Thin Films: Controlled Porosity, Largely Enhanced Luminous Transmittance and Solar Modulating Ability

ARTICLE *in* LANGMUIR · FEBRUARY 2014

Impact Factor: 4.46 · DOI: 10.1021/la404666n · Source: PubMed

6 AUTHORS, INCLUDING:

Ning Wang
Nanyang Technological University
39 PUBLICATIONS **465** CITATIONS
SEE PROFILE

Joachim SC Loo
Nanyang Technological University
163 PUBLICATIONS **3,546** CITATIONS
SEE PROFILE

Yi Long
Nanyang Technological University
27 PUBLICATIONS **177** CITATIONS
SEE PROFILE

Langmuir

Article

pubs.acs.org/Langmuir

Nanoporous Thermochromic VO_2 (M) Thin Films: Controlled Porosity, Largely Enhanced Luminous Transmittance and Solar Modulating Ability

Xun Cao,[†] Ning Wang,[†] Jia Yan Law,[†,‡] Say Chye Joachim Loo,[†] Shlomo Magdassi,[§] and Yi Long*[,†]

[†]School of Materials Science and Engineering and [‡]Facility for Analysis, Characterization, Testing and Simulation, Nanyang Technological University, 50 Nanyang Avenue, Singapore 639798

[§]Casali Institute of Applied Chemistry, Edmund Safra Campus, The Hebrew University, Jerusalem, Israel 91904

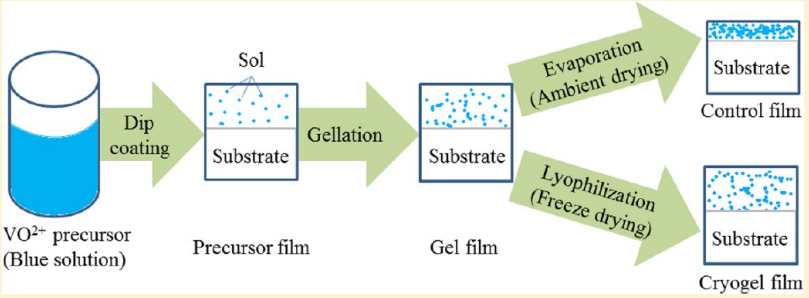

ABSTRACT: Vanadium dioxide is the most widely researched thermochromic material with a phase transition temperature (τ_c) of around 68 °C, and its thermochromic performance can be enhanced by adding nanoporosity. Freeze-drying has been employed to fabricate nanostructures with different porosities from 16 to 45% by varying the prefreezing temperature and precursor concentration. The luminous transmittance (T_{lum}) and solar modulating ability (ΔT_{sol}) are greatly enhanced as a result of increasing pore size and pore density. The freeze-dried sample with 7.5 mL of H_2O_2 precursor dip-coated at 300 mm/min gives the best combination of thermochromic properties ($T_{lum} \approx 50\%$, $\Delta T_{sol} = 14.7\%$), which surpasses the best combined thermochromic performance reported to date that we are aware of ($T_{lum} \approx 41\%$, $\Delta T_{sol} = 14.1\%$).

1. INTRODUCTION

Vanadium dioxide (VO_2) exhibits a fully reversible transition from an insulating monoclinic phase ($P2_1/c$) to a metallic rutile phase ($P4_2/mnm$) at around 68 °C.[1] The metal−insulator transition (MIT) can be characterized by the dramatic change in the optical properties of VO_2 thin films.[2] When numerous dopants are introduced into its crystal lattice via various methods, VO_2 is able to transit the phase at around room temperature ($\tau_c \approx 25$ °C),[3] hence becoming an ideal choice as the coating material for smart windows.[4−7] For practical applications, the major challenge for VO_2-based coatings is to improve the luminous transmittance (T_{lum}) and solar modulating ability (the ability to regulate the input solar energy, ΔT_{sol}) simultaneously.[8]

Among the reported methods, only a few can achieve enhanced T_{lum} with little sacrifice of ΔT_{sol}. Some of the reported methods include doping certain ions (such as Mg^{2+} and Eu^{3+}) into the VO_2 crystal lattice,[9,10] fabricating a multilayered structure ($TiO_2/VO_2/TiO_2/VO_2/TiO_2$),[11] and applying antireflection (AR) coatings, such as TiO_2 and Si−Al gel top layers.[12−14] It was proposed that pores with air can be considered to be a secondary component, thus nanoporous VO_2 films could enhance both T_{lum} and ΔT_{sol} by increasing the density of pores.[15] This was confirmed by Kang et al.,[16] who used polymer-assisted deposition to produce a nanoporous film with an ∼28 nm mean pore size, and gave one of the best reported results ($T_{lum} \approx 41\%$, $\Delta T_{sol} = 14.1\%$) in the literature as shown in Table 1. The fabrication of periodic porous structure and the use of the sol−gel method followed by evaporation have also been reported to produce nanoporous structures with improved properties, and their properties are listed in Table 1. When sols are frozen at low temperature and

Table 1. Summary of Ways to Fabricate Nanoporous VO_2 Thin Films and Their Optical Properties

synthesis method	T_{lum}	ΔT_{sol}	mean pore size
polymer-assisted deposition[a,16]	∼41%	14.1%	28 nm
sol−gel[24] (V_2O_5-H_2O_2 precursor)	∼40%	2.2%	elongated pores surrounded at grain boundaries, ∼100 nm in width
solution infiltration[25] (periodic porous structure)	70.2%	7.9%	∼200 nm
sol−gel[26] (CTAV-BuOH precursor)	46.5%	unreported	∼500 nm

[a]This is the best reported combination of thermochromic properties prior to this report.

dx.doi.org/10.1021/la404666n | Langmuir XXXX, XXX, XXX−XXX

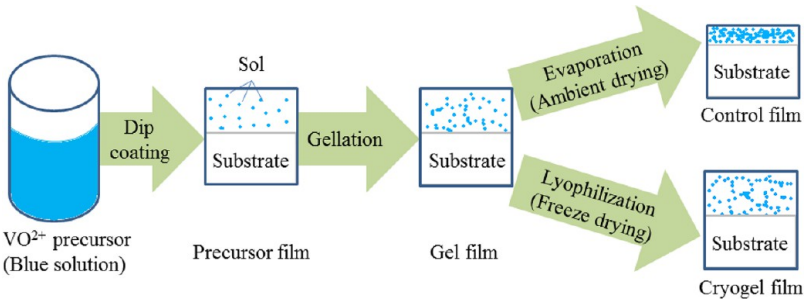

Figure 1. Schematic flowchart (side view, not to scale) for the synthesis of a control sample via evaporation (ambient drying) and nanoporous samples via lyophilization (freeze-drying).

low pressure, solvents will sublime and be removed by vacuum to produce as-obtained nanoporous SiO_2 and Al_2O_3 cryogels via lyophilization (freeze-drying).[17−23] Freeze-drying is widely used in chemical synthesis and the food-processing industry; therefore, it is readily scalable. In this study, we report a facile method of fabricating nanoporous VO_2 (M) thin films with the best thermochromic properties ($T_{lum} \approx 50\%$, $\Delta T_{sol} = 14.7\%$) via the dip-coating of solution precursors followed by the lyophilization of samples.

2. EXPERIMENTAL SECTION

The chemicals used in this study were vanadium(V) oxide (V_2O_5, 99.99%, Alfa Aesar), hydrogen peroxide (H_2O_2, 30 wt %, VWR), and oxalic acid dihydrate ($(COOH)_2{\cdot}2H_2O$, 99.5%, VWR). All of the above-mentioned chemicals were used as received without any further purification.

Figure 1 shows a schematic flowchart (not to scale) for the synthesis of nanoporous thin film samples through lyophilization and control samples via evaporation. The powder precursors were dissolved in solution to form sol followed by gelation to form a more rigid structure, and the solution was dip-coated onto the fused silica substrates. The solvent between the gels was evaporated at room temperature to obtain the control sample and freeze-dried to obtain large-pore structures.

2.1. Synthesis of Coatings. V_2O_5 powder (182 mg) was dissolved in different volumes (7.5, 10.0, 12.5, 15.0, and 17.5 mL) of H_2O_2 and vigorously stirred at 70 °C. When a reddish-brown sol was formed, 400 mg of oxalic acid was added. The mixture was continuously stirred until a clear blue solution of VO^{2+} was obtained.[27] The as-obtained solution was filtered to remove any undissolved oxalic acid. The final precursor was dip-coated onto a 15 × 15 × 0.5 mm^3 precleaned fused silica substrate using a dip coater (KSV Instruments Limited) at various withdrawal rates (100, 200, and 300 mm/min). After the sample was dried under ambient conditions, one side of the coating was carefully wiped off using a wet cotton bud.

2.2. Freeze-Drying of Thin Films. The single-side-coated thin film was contained in a 50 mL centrifuge tube (Corning Inc.), which was covered with a piece of filter paper and sealed using parafilm. It was then placed in a 300 mL freeze-drying flask (Fisher Scientific) and frozen in a freezer (MDF-U537, Sanyo) at various temperatures (−20 and −30 °C) for 3 h before being loaded onto the lyophilizer (FreeZone 2.5 Plus, Labconco) for 24 h of freeze-drying. The lyophilizer collector was set at −80 °C and 0.01 mbar.

2.3. Heat Treatment of Samples. After being freeze-dried, the sample was immediately removed from the centrifuge tube and annealed at 550 °C for 2 h in a tube furnace containing an argon (99.9995%, NOX) atmosphere.[10] The ramping rate was set to 1.0 °C/min, and the gas flow rate was tuned to around 200 cm^3/min. The as-obtained VO_2 thin films were light bronze in color.

2.4. Characterization Method. The XRD patterns were examined using a Shimadzu XRD-6000 X-ray diffractometer (Cu Kα, λ = 0.15406 nm produced under a 40 kV voltage and a 30 mA current) at an X-ray grazing angle of 1.0°. The surface morphologies of the samples were viewed under a JEOL JSM-6340F field-emission scanning electron microscope (FESEM, accelerating voltage 5 kV). The porosity based on FESEM images was calculated using Origin Pro 9. The transmission electron microscopy (TEM) image and selected area electron diffraction (SAED) pattern were obtained using a Carl Zeiss LIBRA 120 in-column energy filter TEM (accelerating voltage 120 kV) equipped with an integrated Omega filter. The transmittance and reflectance spectra were collected using an Agilent Cary 5000 UV−vis−NIR spectrophotometer, which was equipped with a Linkam PE120 system Peltier simple heating and cooling stage for the former and a diffuse reflectance accessory (DRA) for the latter. The calculations of integrated luminous transmittance (T_{lum}, $280 \le \lambda \le 780$ nm) and solar transmittance (ΔT_{sol}, $250 \le \lambda \le 2500$ nm) can be found in an earlier publication.[28] The thickness was measured on a KLA-Tencor Alpha-Step IQ surface profiler, and the recorded value was averaged from five measured points with ∼20% variation due to the nonuniformity of the dip-coated samples. A simple cross-cut test (ASTM 3359-08) has been performed to test the coating adhesion, and the results show that the sintered samples are classified as 5B, which indicates excellent adhesion to the substrate as a result of the high-temperature annealing.

3. RESULTS AND DISCUSSION

3.1. Effects of Prefreezing and Freeze-Drying on Thermochromic Properties. The samples were dip-coated using the precursor with 15.0 mL of H_2O_2 at a withdrawal rate of 100 mm/min and were prefrozen at different temperatures (−20 or −30 °C) for 3 h. The XRD patterns revealed a peak at $2\theta \approx 28.0°$, as shown in Figure 2, that can be ascribed to the (011) plane of monoclinic VO_2 (JCPDS no. 82-661). The grain size is estimated to be ∼91 nm using the Debye−Scherrer method. Different prefreezing temperatures and freeze-drying processes have no influence on the phase formation compared to that of control samples. The formation of a pure VO_2 (M) phase by oxalic acid reduction is similar to that in the literature in the absence of acid in the precursor.[29−31]

The transmittance and reflectance spectra are shown in Figure 3. In contrast to the control sample, freeze-drying increases the transmittance at all wavelengths (250−2500 nm) at both 20 and 90 °C, which is reflected in enhanced T_{lum} and T_{sol} (Table 2). For samples without prefreezing, transmittance within the visible range (380−780 nm) at 20 °C is generally lower than that at 90 °C; as the prefreezing temperature decreases, the intersection point (inset of Figure 3a) of the two spectra shows a blue shift and T_{lum} at 20 °C exceeds that at 90 °C. This reveals a similar trend to that of the interference effect,[32] which leads to an increase in ΔT_{lum}, thereby giving a higher ΔT_{sol} (Table 2).[16]

Correspondingly, Figure 3b reveals a relatively low reflectance within the UV−vis−NIR region, indicating that the as-synthesized VO_2 thin films have a high transparency at

dx.doi.org/10.1021/la404666n | Langmuir XXXX, XXX, XXX−XXX

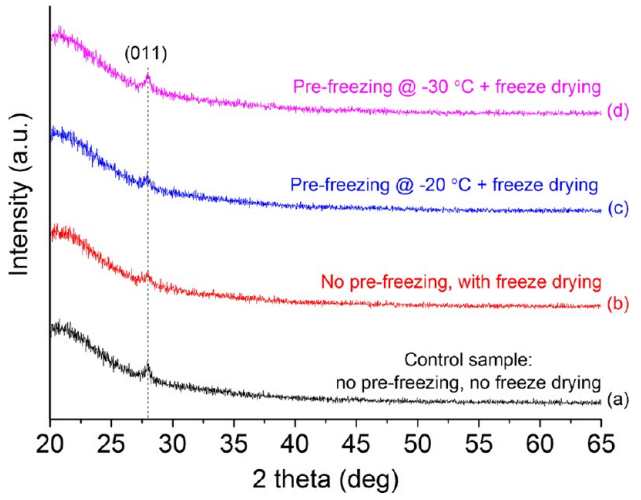

Figure 2. XRD patterns of samples coated using 15.0 mL of H_2O_2 precursor: (a) control, without prefreezing and freeze-drying, (b) freeze-drying without prefreezing, (c) prefrozen at −20 °C followed by freeze-drying, and (d) prefrozen at −30 °C followed by freeze-drying.

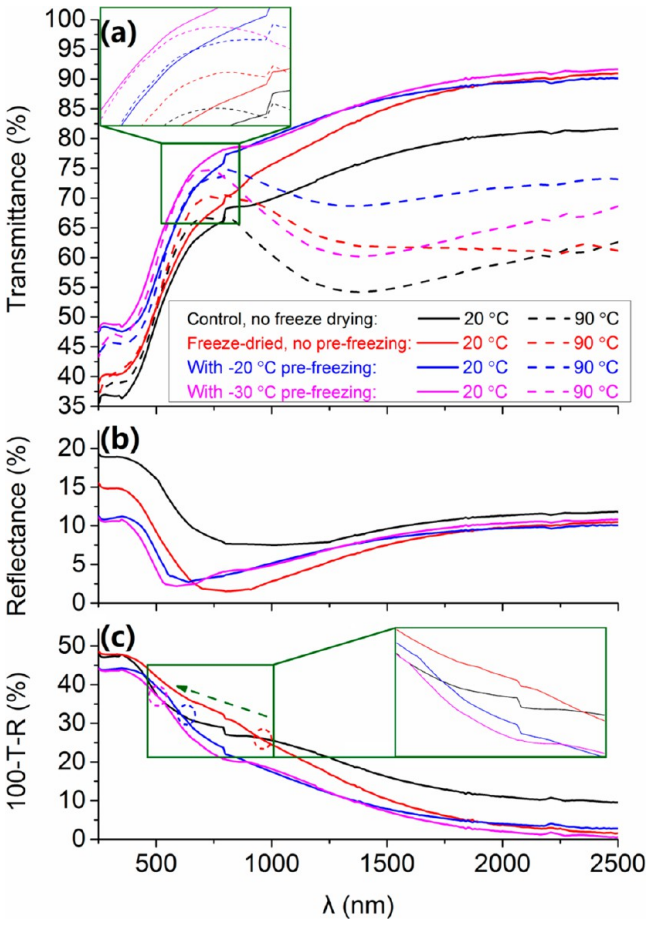

Figure 3. (a) Transmittance, (b) reflectance, and (c) $1 - T\% - R\%$ spectra of the control (black lines); freeze-drying without prefreezing (red lines); with −20 °C prefreezing (blue lines) and −30 °C prefreezing (purple lines) samples coated using 15.0 mL of H_2O_2 precursor. Transmittance spectra were collected at both 20 and 90 °C, but reflectance spectra were collected only at 20 °C.

20 °C. Compared to the control sample (black line), all of the freeze-dried samples have a lower reflection (R) from λ = 250 to 2500 nm, which indicates that the reflection could be reduced by increasing the porosity. This is mainly due to the fact that with the reduced refractive index (n) of the porous films a lower R could be expected according to the Fresnel equation $R = (n - 1)/(n + 1)^2$. The reflectance valleys depict a blue shift (from the NIR region to the visible region) as a result of freeze-drying and a decreasing prefreezing temperature, which in turn confirms that freeze-drying after a suitable prefreezing temperature could lead to an enhancement in T_{lum}. Figure 3c shows that all of the freeze-dried samples have lower absorption at λ > 800 nm than the control sample. The more porous films (prefrozen at −20 °C and −30 °C, in blue and purple, respectively) show lower absorption at λ > 600 nm. The difference between these two samples and the control is small at λ < 600 nm, which may be due to the subsurface and/or intergranular scattering effect induced by porosity. It is interesting that the intersection point (where the absorption of freeze-dried samples starts to be less than that of the control sample) exhibits a blue shift that shows that with increasing porosity, less absorption would occur as a result of the decreased absorption coefficient.[33,34] The high transmittance in Figure 3a, low reflectance valleys in Figure 3b, and low absorption in Figure 3c prove that prefreezing and freeze-drying processes reduce the absorption effect and reflection of VO_2 thin films in the visible range, which generate the increasing trend in T_{lum} as listed in Table 2.

Prefreezing improves the transmittance in the UV and visible range (250−780 nm), which is in agreement with the calculated T_{lum} values (Table 2). When the prefreezing temperature is lowered, T_{lum} shows an increasing trend; this might be due to the fact that with prefreezing at lower temperature, the grains and pores of VO_2 tend to grow larger (Figure 4) and the calculated porosities are 2, 9, 20, and 33% for the control, nonprefrozen, −20 °C prefrozen, and −30 °C prefrozen samples, respectively. It is interesting that with lower prefreezing temperatures T_{sol} (90 °C) remains nearly the same (64.3, 65.8, and 65.0%), whereas T_{sol} (20 °C) increases from 68.5 to 70.8 to 72.9%, which suggests that with increasing porosity T_{sol} (20 °C) is more favorably enhanced compared to T_{sol} (90 °C), giving rise to increased ΔT_{sol}. This observation is consistent with the simulation results.[16] Because of freeze-drying, a large amount of solvent could be removed with good preservation of the intergrain porous microstructures (Figure 4).[22] Light penetrates more easily through a medium with a lower refractive index, which in this case is air (pores), hence leading to a much higher transmittance in the freeze-dried samples (Table 2).[15,35,36]

3.2. Effects of Precursor Concentration and Withdrawal Rate on the Thermochromic Properties. The precursor concentration was modified by changing the solvent (H_2O_2) volume from 7.5 to 17.5 mL to study the porosity effects on thermochromism at a fixed withdrawal rate of 100 mm/min. The thermochromic properties of the samples are summarized in Table 3. When the solvent content decreases and the viscosity increases, T_{lum} and T_{sol} at both temperatures (20 and 90 °C) decrease with higher ΔT_{sol} for control samples mainly because of the increased thickness. Similar trends are observed in freeze-dried samples with a less-steep decrease in averaged T_{lum} and a steeper increase in ΔT_{sol} than for the control samples, and this would suggest that freeze-drying has more predominant effect than thickness in improving both T_{lum} and ΔT_{sol} (Figure 5a). Freeze-dried samples have higher T_{lum}, T_{sol}, ΔT_{lum}, and ΔT_{sol} than respective control samples; this

dx.doi.org/10.1021/la404666n | Langmuir XXXX, XXX, XXX−XXX

Table 2. Effects of Prefreezing and Freeze Drying on the Thermochromic Properties of Thin Films

prefreezing temperature (°C)	freeze-drying	T_{lum} (20/90 °C)	ΔT_{lum}	T_{sol} (20/90 °C)	ΔT_{sol}	porosity
none[a]	none	55.2%/58.2%	−3.0%	61.8%/58.9%	2.9%	2%
none	yes	63.0%/62.6%	0.4%	68.5%/64.3%	4.2%	9%
−20	yes	67.2%/66.2%	1.0%	70.8%/65.8%	5.0%	20%
−30	yes	71.1%/70.2%	0.9%	72.9%/65.0%	7.9%	33%

[a]This is the control sample with the conventional evaporation drying method.

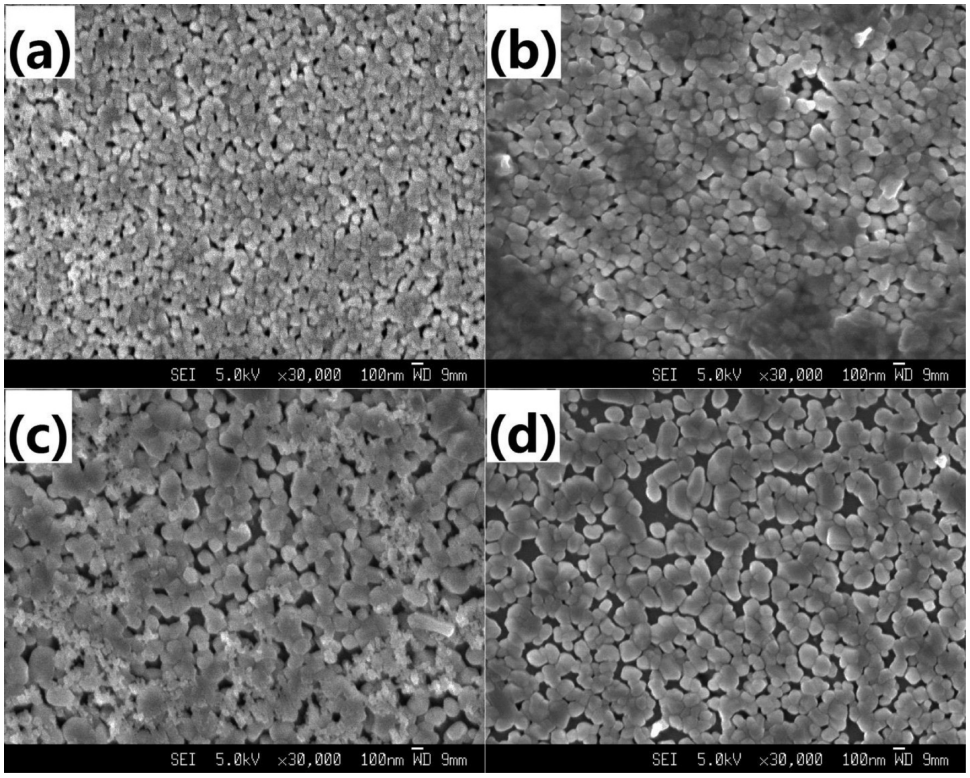

Figure 4. FESEM images of samples coated using 15.0 mL of H_2O_2 precursor: (a) control, without prefreezing and freeze-drying, (b) freeze-dried without prefreezing, (c) prefrozen at −20 °C followed by freeze-drying, and (d) prefrozen at −30 °C followed by freeze-drying.

Table 3. Effect of Precursor Concentration on Thermochromic Properties of Thin Films

H_2O_2 volume (mL)	sample type	T_{lum} (20/90 °C)	ΔT_{lum}	T_{sol} (20/90 °C)	ΔT_{sol}	thickness (nm)
7.5	control	50.6%/52.1%	−1.5%	58.6%/53.7%	4.9%	54.0
	freeze-dried	**60.1%/58.6%**	**1.5%**	**59.0%/46.5%**	**12.5%**	**57.0**
10.0	control	54.0%/55.3%	−1.3%	62.0%/57.2%	4.8%	52.0
	freeze-dried	60.9%/59.9%	1.0%	69.5%/60.0%	9.5%	49.5
12.5	control	55.5%/55.4%	0.1%	61.5%/56.9%	4.6%	44.0
	freeze-dried	60.6%/59.3%	1.3%	67.8%/59.4%	8.4%	47.0
15.0	control	55.2%/58.2%	−3.0%	61.7%/58.8%	2.9%	41.5
	freeze-dried	71.1%/70.2%	0.9%	72.9%/65.0%	7.9%	41.5
17.5	control	68.7%/70.0%	−1.3%	72.4%/70.3%	2.1%	33.0
	freeze-dried	71.6%/71.4%	0.2%	76.1%/70.5%	5.6%	39.0

observation is consistent with the prefreezing temperature effect as discussed in section 3.1. This could be mainly due to the fact that in less concentrated precursor, more H_2O produced during synthesis would be frozen and sublimed to form larger pores, which can be confirmed by Figure 6a,b as the porosities of samples increased from 16% (7.5 mL of H_2O_2) to 44% (17.5 mL of H_2O_2). The large pore in the sample with 17.5 mL of H_2O_2 is further observed in the TEM image (Figure 6c), and the inserted diffraction pattern confirms the formation of the VO_2 (M) phase as shown in the XRD (Figure 2). The diffraction rings indicate that the as-deposited samples are polycrystalline. The highest ΔT_{sol} of 12.5% can be obtained with 7.5% H_2O_2 as highlighted in Table 3.

To improve ΔT_{sol} further, the thicknesses were varied by changing the withdrawal rate from 100 to 300 mm/min using 7.5 mL of H_2O_2 precursor. Table 4 and Figure 5b show that when the withdrawal rate increases, higher ΔT_{sol} can be obtained with a depression in T_{lum} as a result of film thickening for both control and freeze-dried samples.[32] Freeze-drying can increase T_{lum} and ΔT_{lum}, thus largely improving ΔT_{sol} (Figure

dx.doi.org/10.1021/la404666n | Langmuir XXXX, XXX, XXX−XXX

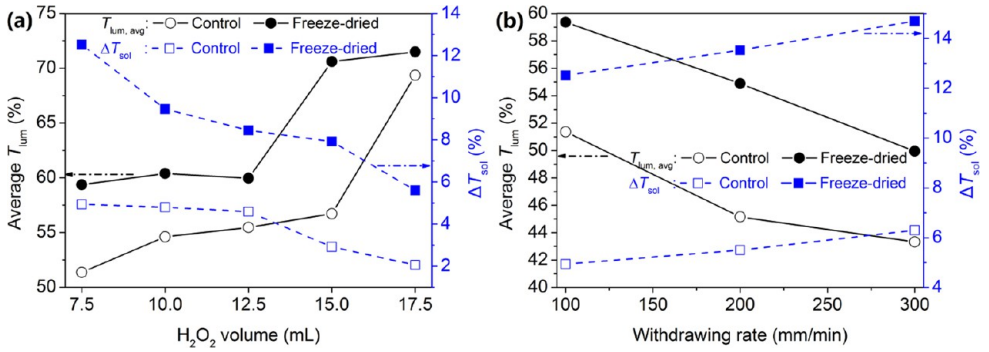

Figure 5. Effect of (a) precursor concentration and (b) withdrawal rate on the thermochromic properties of thin films. The average T_{lum} is the average value of T_{lum} (20 °C) and T_{lum} (90 °C).

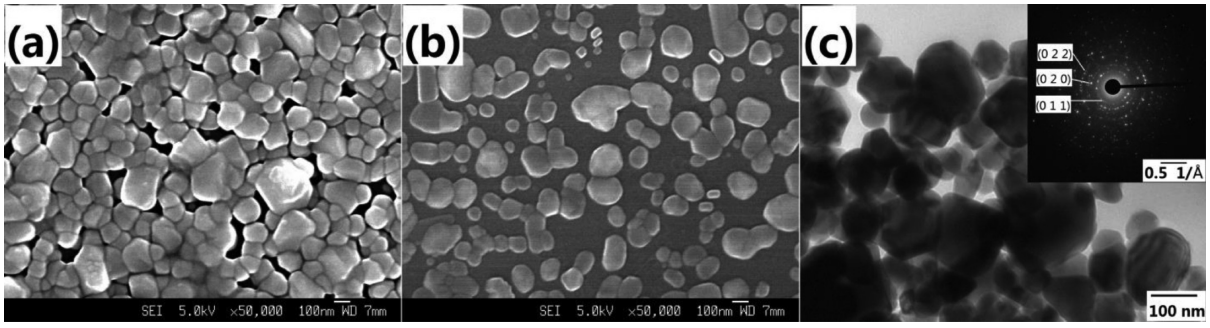

Figure 6. FESEM images of freeze-dried samples with (a) 7.5 and (b) 17.5 mL of H_2O_2. (c) TEM image and (inset) SAED pattern of freeze-dried sample with 17.5 mL of H_2O_2.

Table 4. Effect of Coating-Speed-Controlled Thickness on Thermochromic Properties of Thin Films

withdrawing rate (mm/min)	sample type	T_{lum} (20/90 °C)	ΔT_{lum}	T_{sol} (20/90 °C)	ΔT_{sol}	thickness (nm)
100	control	50.6%/52.1%	−1.5%	58.6%/53.7%	4.9%	54.0
	freeze-dried	60.1%/58.6%	1.5%	59.0%/46.5%	12.5%	57.0
200	control	46.4%/47.9%	−1.5%	50.9%/45.4%	5.5%	82.0
	freeze-dried	55.9%/53.9%	2.0%	53.8%/40.3%	13.5%	95.5
300	control	42.6%/44.1%	−1.5%	53.7%/47.4%	6.3%	113.0
	freeze-dried	**50.6%/49.4%**	**1.2%**	**58.9%/44.2%**	**14.7%**	**120.0**

5b) compared to that of control samples. The highlighted data in Table 4 shows the best combination of thermochromic properties that gives an ∼20% increase in T_{lum} (∼50 vs 41%) and a slightly higher ΔT_{sol} (14.7 vs 14.1%) compared to the best reported results in the literature.[16]

4. CONCLUSIONS

In this study, VO_2 (M) thin films were synthesized by the dip-coating of VO^{2+} solution followed by freeze-drying, which rendered nanoporous structures with excellent thermochromic properties. By varying the prefreezing temperature and tailoring the vanadium concentration and coating thickness of the freeze-dried porous VO_2 coatings, T_{lum} and ΔT_{sol} can be tuned between 50.0 to 71.6% and from 5.6 to 14.7%, respectively. An interference effect that contributed largely to the enhanced ΔT_{lum} and ΔT_{sol} with the introduction of intergrain pores was observed. Freeze-drying enhances both T_{lum} and ΔT_{sol} simultaneously compared to the same parameters for control samples and produces the most competitive result ($T_{lum} \approx$ 50.0%, ΔT_{sol} = 14.7%) in the literature.

AUTHOR INFORMATION

Corresponding Author

*E-mail: longyi@ntu.edu.sg.

Author Contributions

X.C. and N.W. contributed equally.

ACKNOWLEDGMENTS

This research is supported by the Singapore National Research Foundation under the CREATE Programme: Nanomaterials for Energy and Water Management. The XRD, FESEM, and TEM characterizations were performed at the Facility for Analysis, Characterization, Testing and Simulation (FACTS) at Nanyang Technological University, Singapore.

REFERENCES

(1) Goodenough, J. B. The Two Components of the Crystallographic Transition in VO_2. *J. Solid State Chem.* **1971**, *3*, 490−500.

(2) Petrov, G. I.; Yakovlev, V. V.; Squier, J. A. Nonlinear Optical Microscopy Analysis of Ultrafast Phase Transformation in Vanadium Dioxide. *Opt. Lett.* **2002**, *27*, 655−657.

(3) Kiri, P.; Hyett, G.; Binions, R. Solid State Thermochromic Materials. *Adv. Mater. Lett.* **2010**, *1*, 86−105.

dx.doi.org/10.1021/la404666n | *Langmuir* XXXX, XXX, XXX−XXX

(4) Zhang, Z. T.; Gao, Y. F.; Chen, Z.; Du, J.; Cao, C. X.; Kang, L. T.; Luo, H. J. Thermochromic VO_2 Thin Films: Solution-Based Processing, Improved Optical Properties, and Lowered Phase Transformation Temperature. *Langmuir* **2010**, *26*, 10738−10744.
(5) Batista, C.; Ribeiro, R. M.; Teixeira, V. Synthesis and Characterization of VO_2-Based Thermochromic Thin Films for Energy-Efficient Windows. *Nanoscale Res. Lett.* **2011**, *6*, 301.
(6) Xiao, X. D.; Cheng, H. L.; Dong, G. P.; Yu, Y. G.; Chen, L. H.; Miao, L.; Xu, G. A Facile Process to Prepare One Dimension VO_2 Nanostructures with Superior Metal-Semiconductor Transition. *CrystEngComm* **2013**, *15*, 1095−1106.
(7) Manning, T. D.; Parkin, I. P.; Pemble, M. E.; Sheel, D.; Vernardou, D. Intelligent Window Coatings: Atmospheric Pressure Chemical Vapor Deposition of Tungsten-Doped Vanadium Dioxide. *Chem. Mater.* **2004**, *16*, 744−749.
(8) Granqvist, C. G. Transparent Conductors as Solar Energy Materials: A Panoramic Review. *Sol. Energy Mater. Sol. Cells* **2007**, *91*, 1529−1598.
(9) Mlyuka, N. R.; Niklasson, G. A.; Granqvist, C. G. Mg Doping of Thermochromic VO_2 Films Enhances the Optical Transmittance and Decreases the Metal-Insulator Transition Temperature. *Appl. Phys. Lett.* **2009**, *95*, 171909.
(10) Cao, X.; Wang, N.; Magdassi, S.; Mandler, D.; Long, Y. Europium Doped Vanadium Dioxide Material: Reduced Phase Transition Temperature, Enhanced Luminous Transmittance and Solar Modulation. *Sci. Adv. Mater.* **2014**, *6*, 1−4.
(11) Granqvist, C. G.; Lansaker, P. C.; Mlyuka, N. R.; Niklasson, G. A.; Avendano, E. Progress in Chromogenics: New Results for Electrochromic and Thermochromic Materials and Devices. *Sol. Energy Mater. Sol. Cells* **2009**, *93*, 2032−2039.
(12) Burkhardt, W.; Christmann, T.; Meyer, B. K.; Niessner, W.; Schalch, D.; Scharmann, A. W- and F-Doped VO_2 Films Studied by Photoelectron Spectrometry. *Thin Solid Films* **1999**, *345* (), 229−235.
(13) Jin, P.; Xu, G.; Tazawa, M.; Yoshimura, K. A VO_2-Based Multifunctional Window with Highly Improved Luminous Transmittance. *Jpn. J. Appl. Phys.* **2002**, *41*, L278−L280.
(14) Liu, C.; Wang, N.; Long, Y. Multifunctional Overcoats on Vanadium Dioxide Thermochromic Thin Films with Enhanced Luminous Transmission and Solar Modulation, Hydrophobicity and Anti-Oxidation. *Appl. Surf. Sci.* **2013**, *283*, 222−226.
(15) Jin, P. Japenese Patent 2007171759-A, July 5, 2007.
(16) Kang, L. T.; Gao, Y. F.; Luo, H. J.; Chen, Z.; Du, J.; Zhang, Z. T. Nanoporous Thermochromic VO_2 Films with Low Optical Constants, Enhanced Luminous Transmittance and Thermochromic Properties. *ACS Appl. Mater. Interfaces* **2011**, *3*, 135−138.
(17) Su, L. F.; Miao, L.; Tanemura, S.; Xu, G. Low-Cost and Fast Synthesis of Nanoporous Silica Cryogels for Thermal Insulation Applications. *Sci. Technol. Adv. Mater.* **2012**, *13*, 035003.
(18) Shlyakhtin, O.; Oh, Y.-J. Inorganic Cryogels for Energy Saving and Conversion. *J. Electroceram.* **2009**, *23*, 452−461.
(19) Mukai, S.; Nishihara, H.; Tamon, H. Porous Microfibers and Microhoneycombs Synthesized by Ice Templating. *Catal. Surv. Asia* **2006**, *10*, 161−171.
(20) Baudrin, E.; Sudant, G.; Larcher, D.; Dunn, B.; Tarascon, J.-M. Preparation of Nanotextured VO_2[B] from Vanadium Oxide Aerogels. *Chem. Mater.* **2006**, *18*, 4369−4374.
(21) Sudant, G.; Baudrin, E.; Dunn, B.; Tarascon, J.-M. Synthesis and Electrochemical Properties of Vanadium Oxide Aerogels Prepared by a Freeze-Drying Process. *J. Electrochem. Soc.* **2004**, *151*, A666−A671.
(22) Xu, J. J.; Yang, J. Nanostructured Amorphous Manganese Oxide Cryogel as a High-Rate Lithium Intercalation Host. *Electrochem. Commun.* **2003**, *5*, 230−235.
(23) Harreld, J. H.; Dong, W.; Dunn, B. Ambient Pressure Synthesis of Aerogel-Like Vanadium Oxide and Molybdenum Oxide. *Mater. Res. Bull.* **1998**, *33*, 561−567.
(24) Wang, N.; Huang, Y. Z.; Magdassi, S.; Mandler, D.; Liu, H.; Long, Y. Formation of VO_2 Zero-Dimensional/Nanoporous Layers with Large Supercooling Effects and Enhanced Thermochromic Properties. *RSC Adv.* **2013**, *3*, 7124.
(25) Zhou, M.; Bao, J.; Tao, M. S.; Zhu, R.; Lin, Y. T.; Zhang, X. D.; Xie, Y. Periodic Porous Thermochromic VO_2(M) Films with Enhanced Visible Transmittance. *Chem. Commun.* **2013**, *49*, 6021.
(26) Ding, S. J.; Liu, Z. Q.; Li, D. Z.; Zhao, W.; Wang, Y. M.; Wan, D. Y.; Huang, F. Q. Tunable Assembly of Vanadium Dioxide Nanoparticles to Create Porous Film for Energy-Saving Applications. *ACS Appl. Mater. Interfaces* **2013**, *5*, 1630−1635.
(27) Pan, A. Q.; Zhang, J.-G.; Nie, Z. M.; Cao, G. Z.; Arey, B. W.; Li, G. S.; Liang, S.-Q.; Liu, J. Facile Synthesized Nanorod Structured Vanadium Pentoxide for High-Rate Lithium Batteries. *J. Mater. Chem.* **2010**, *20*, 9193−9199.
(28) Liu, C.; Cao, X.; Kamyshny, A.; Law, J. Y.; Magdassi, S.; Long, Y. VO_2/Si-Al Gel Nanocomposite Thermochromic Smart Foils: Largely Enhanced Luminous Transmittance and Solar Modulation. *J. Colloid Interface Sci.*, in press, DOI: http://dx.doi.org/10.1016/j.jcis.2013.11.028.
(29) Wang, N.; Magdassi, S.; Mandler, D.; Long, Y. Simple Sol−Gel Process and One-Step Annealing of Vanadium Dioxide Thin Films: Synthesis and Thermochromic Properties. *Thin Solid Films* **2013**, *534*, 594−598.
(30) Rouse, J. H.; Ferguson, G. S. Preparation of Thin Silica Films with Controlled Thickness and Tunable Refractive Index. *J. Am. Chem. Soc.* **2003**, *125*, 15529−15536.
(31) Prevo, B. G.; Hwang, Y.; Velev, O. D. Convective Assembly of Antireflective Silica Coatings with Controlled Thickness and Refractive Index. *Chem. Mater.* **2005**, *17*, 3642−3651.
(32) Xu, G.; Jin, P.; Tazawa, M.; Yoshimura, K. Tailoring of Luminous Transmittance upon Switching for Thermochromic VO_2 Films by Thickness Control. *Jpn. J. Appl. Phys.* **2004**, *43*, 186−187.
(33) Li, S.-Y.; Niklasson, G. A.; Granqvist, C. G. Nanothermochromics: Calculations for VO_2 Nanoparticles in Dielectric Hosts Show Much Improved Luminous Transmittance and Solar Energy Transmittance Modulation. *J. Appl. Phys.* **2010**, *108*, 063525.
(34) Kang, L. T.; Gao, Y. F.; Zhang, Z. T.; Du, J.; Cao, C. X.; Chen, Z.; Luo, H. J. Effects of Annealing Parameters on Optical Properties of Thermochromic VO_2 Films Prepared in Aqueous Solution. *J. Phys. Chem. C* **2010**, *114*, 1901−1911.
(35) Moghal, J.; Reid, S.; Hagerty, L.; Gardener, M.; Wakefield, G. Development of Single Layer Nanoparticle Anti-Reflection Coating for Polymer Substrates. *Thin Solid Films* **2013**, *534*, 541−545.
(36) Moghal, J.; Kobler, J.; Sauer, J.; Best, J.; Gardener, M.; Watt, A. A. R.; Wakefield, G. High-Performance, Single-Layer Antireflective Optical Coatings Comprising Mesoporous Silica Nanoparticles. *ACS Appl. Mater. Interfaces* **2011**, *4*, 854−859.